UNIVERSITY OF OKLAHOMA

Catalytic Upgrading of Vapors and Liquids from Pyrolysis of Biomass

Daniel E. Resasco

Center for Biomass Refining

School of Chemical, Biological and Materials Engineering,

University of Oklahoma,

Norman, OK 73019, USA

U.S. Energy Consumption, 2010

Eq. 46 MM bpd of oil

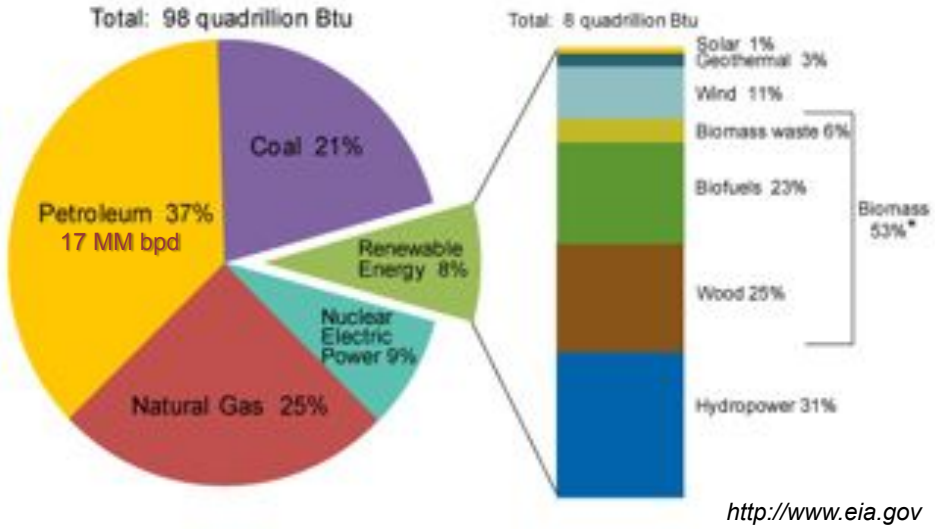

http://www.eia.gov

* Note: Sum of biomass components does not equal 53% due to independent rounding.
Source: U.S. Energy Information Administration, Monthly Energy Review, Table 10.1 (June 2011), preliminary 2010 data.

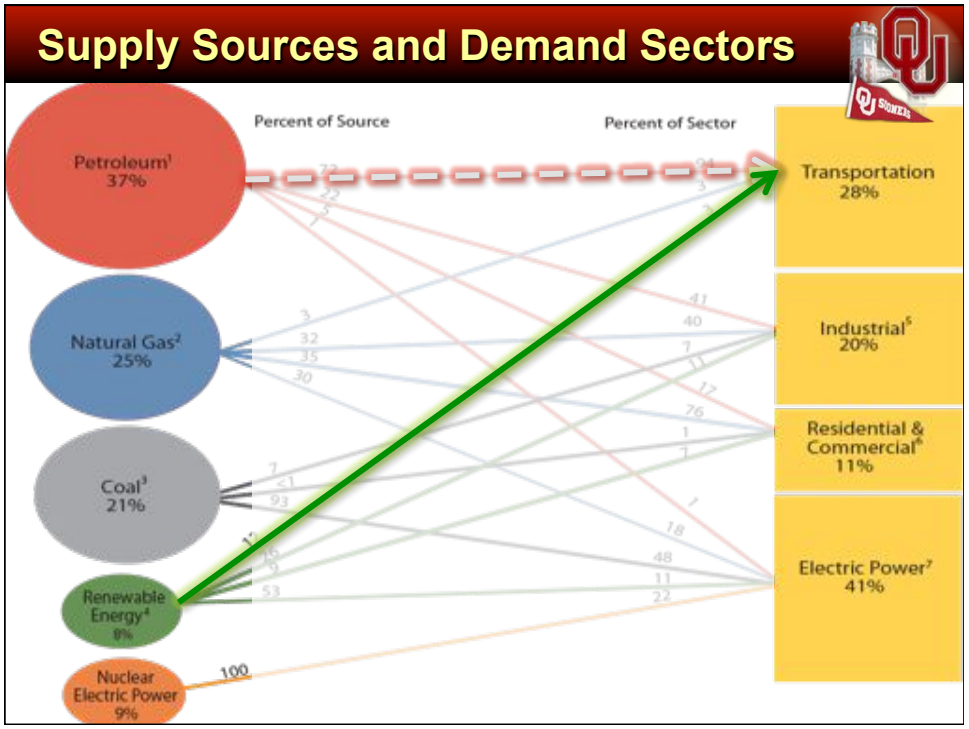
Supply Sources and Demand Sectors
Percent of Source
Percent of Sector
Petroleum[1] 37%
Natural Gas[2] 25%
Coal[3] 21%
Renewable Energy[4] 8%
Nuclear Electric Power 9%
Transportation 28%
Industrial[5] 20%
Residential & Commercial[6] 11%
Electric Power[7] 41%

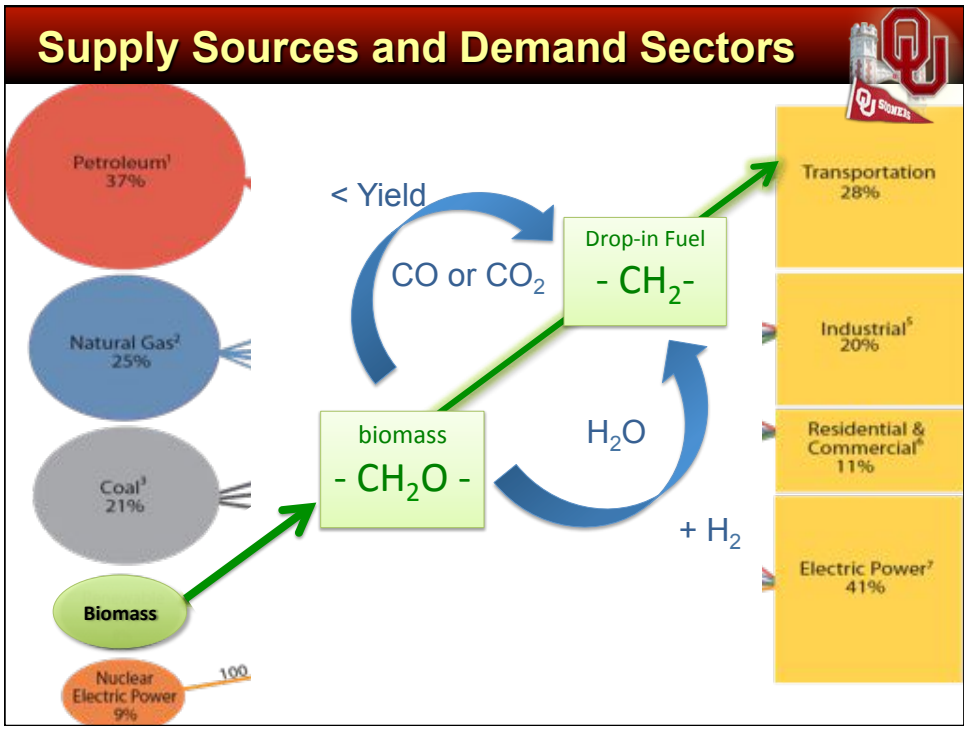
Supply Sources and Demand Sectors
Petroleum[1] 37%
Natural Gas[2] 25%
Coal[3] 21%
Biomass
Nuclear Electric Power 9%
< Yield
CO or CO2
Drop-in Fuel
- CH2-
biomass
- CH2O -
H2O
+ H2
Transportation 28%
Industrial[5] 20%
Residential & Commercial[6] 11%
Electric Power[7] 41%

Lignocellulosic Biomass Conversion

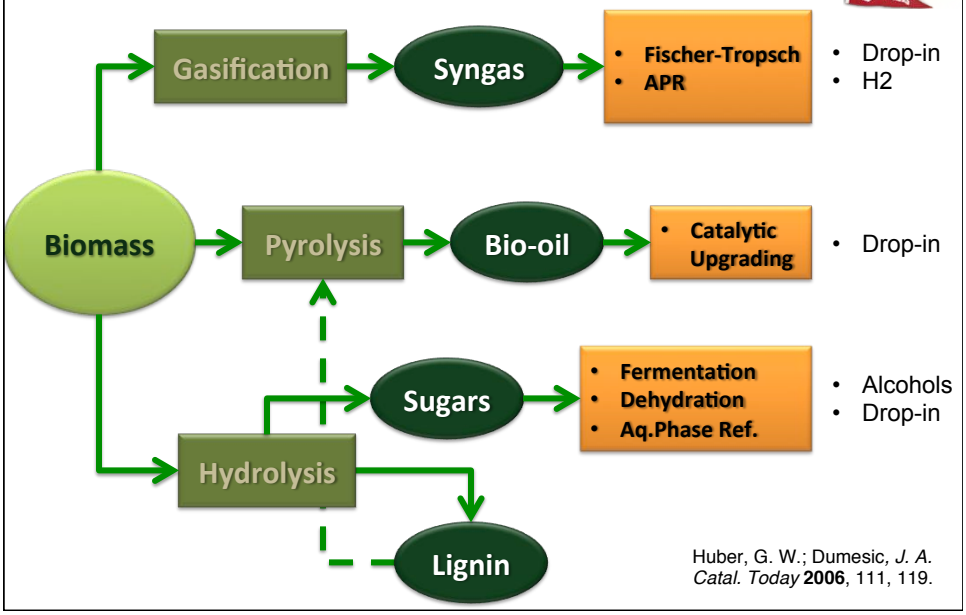

Huber, G. W.; Dumesic, *J. A. Catal. Today* **2006**, 111, 119.

Fast Pyrolysis Products

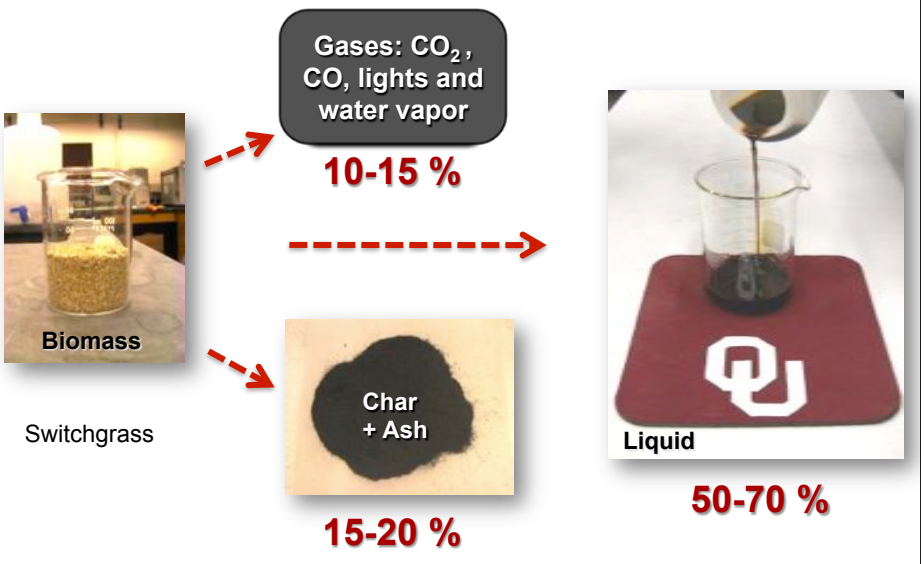

OU Pyrolysis Pilot Unit (Kg-scale)

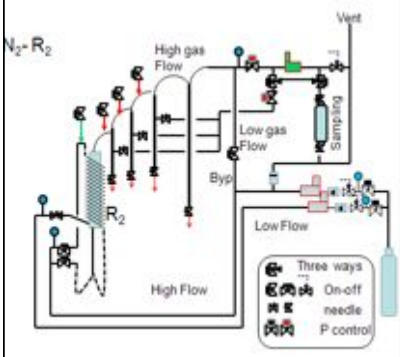

Reactor operating conditions

biomass type:	switchgrass	Fluidized bed material	ground glass
bed particle size	425 -710 µm	Fluidizing gas	N_2
Gas flow rate	3.46 kg/hr	Reactor temperature	500 ˚C
	= 30L/min, 25 ˚C	Biomass feed rate	0.5 kg/hr

OU Pyrolysis Pilot Unit (Kg-scale)

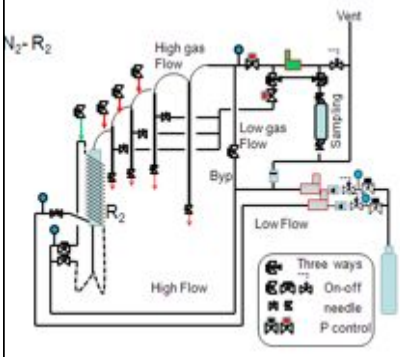

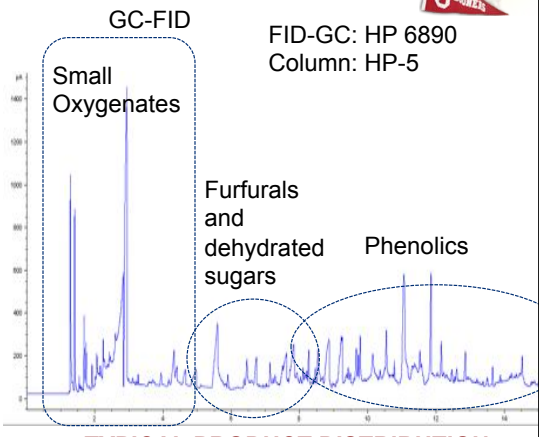

TYPICAL PRODUCT DISTRIBUTION

Reactor operating conditions

biomass type:	switchgrass	Fluidized bed material	ground glass
bed particle size	425 -710 µm	Fluidizing gas	N_2
Gas flow rate	3.46 kg/hr	Reactor temperature	500 ˚C
	= 30L/min, 25 ˚C	Biomass feed rate	0.5 kg/hr

Concept: catalytic cascade to upgrade/refine pyrolysis oil liquids

- **Small oxygenates**
  (aldehydes, alcohols, ketones, acids)
- **Sugar-derived compounds**
  (levoglucosan, furfurals)
- **Lignin-derived phenolics**
  (guaiacol, vanillin, anisole, etc.)

BIOMASS

- CELLULOSE
- HEMICELLULOSE
- LIGNIN

Challenges:
- eliminate excess O
- maximize C retention
- minimize H_2 consumption
- optimize fuel properties
  (from varying feedstocks)
- Catalyst deactivation

Concept: catalytic cascade connected to a multi-stage pyrolysis

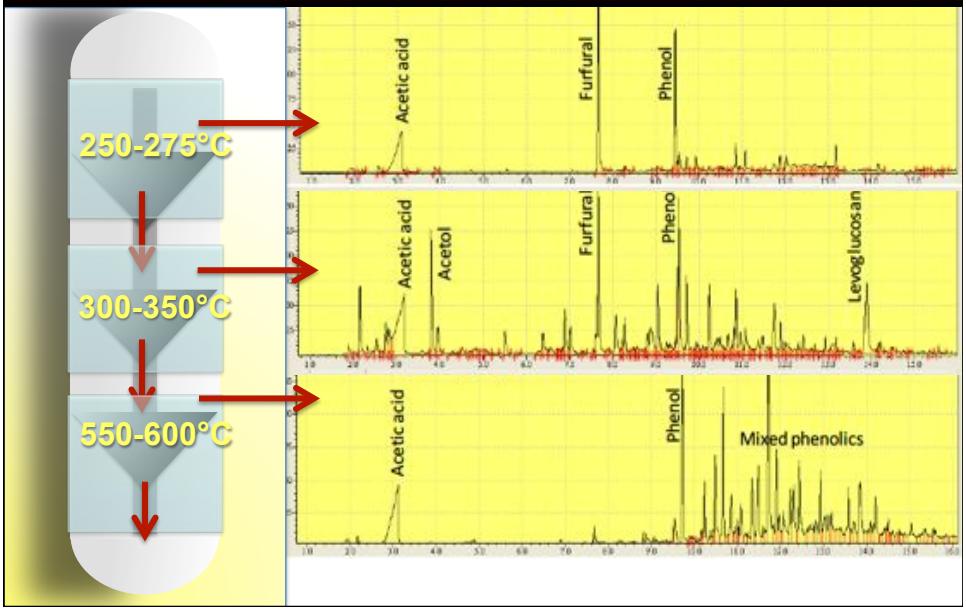

Concept: catalytic cascade connected to a multi-stage pyrolysis

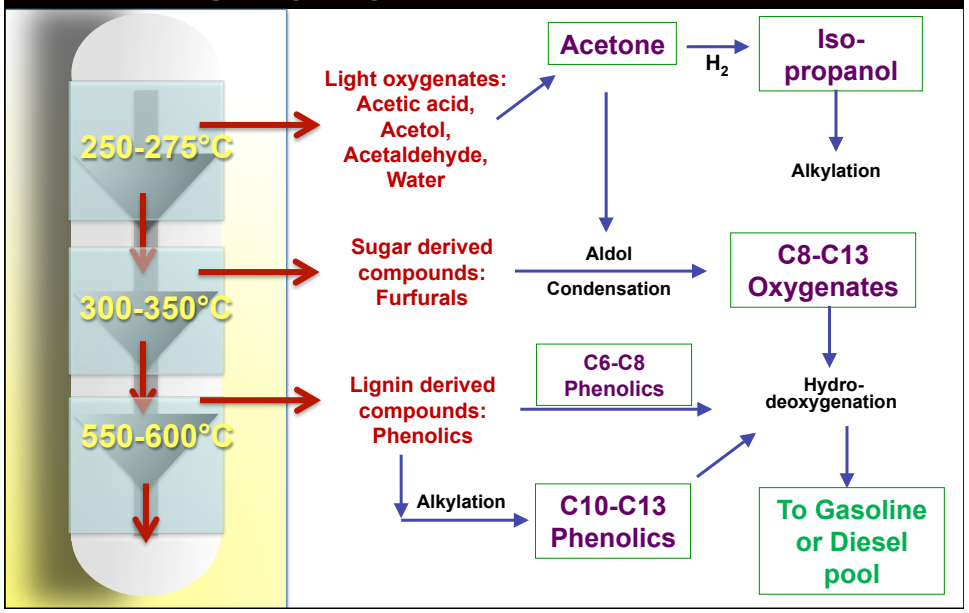

Model Compound Studies

- **Small oxygenates**
  (aldehydes, alcohols, ketones, acids)

Aldol Condensation
Ketonization
Esterification
Aromatization

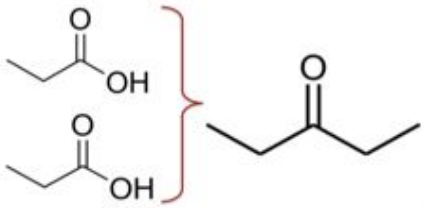

Basic and Acidic Zeolites – Mixed Oxides

Applied Catalysis A, 379 (**2010**) 172 and 385 (**2010**) 80

- **Lignin-derived phenolics**

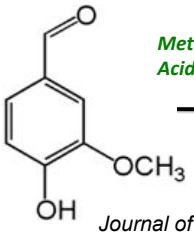

Metals and Acidic Zeolites → BTX

Deoxygenation
Alkylation, Transalkylation

Journal of Catalysis 271 (**2010**) 88–98

Sugar-derived compounds

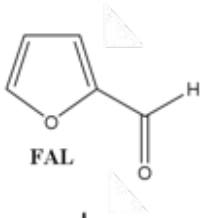

Bases

Aldol Condensation
And Canizarro Reaction

C8 C11 C13

Pd, Ni Ru

Deoxy genation

Diesel

Strategy No. 1
"Building up C-C chains"

Acid-Catalyzed Condensation
and Aromatization of
Small Oxygenates

13

Aromatization of Propanal on H-ZSM5

Initial Concept:

- Oxygenates to Olefins
- Olefins to Oligomers
- Oligomers to Aromatics

Aromatization of Propanal on H-ZSM5

- Aldol Dimerization
- Dehydration
- Aldol Trimerization
- Dehydration
- Enol and Rearrangement
- Aromatization
- Dehydration

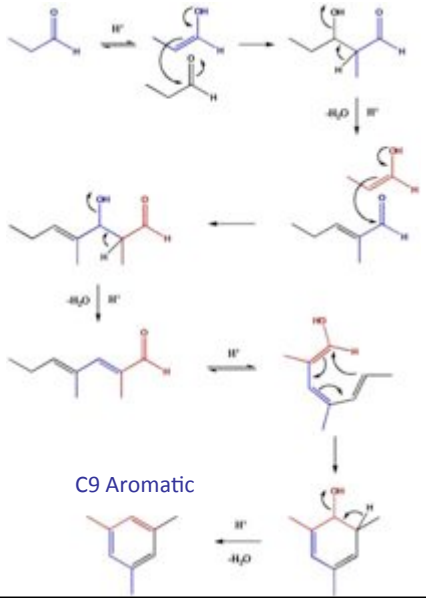

15

Aromatization of Propanal on H-ZSM5

Feed	*Propanal*	*Propylene*	
Conditions	W/F =0.13 h HZSM-5 (45) 400 °C	W/F =4 h HZSM-5 (45) 400°C	W/F =4h HZSM-5 (25) 500°C
Conversion	76	42	66
Gas (C_1-C_3)	32	-	38
isoalkenes (C_4-C_9)	3	42	10
Aromatics	41	1	17

Product Yield Distribution after 60 min on stream in a fixed bed reactor

Journal of Catalysis 271 (**2010**) 201–208

16

Pulses of Propanal on H-ZSM5 produce C9 Aromatics

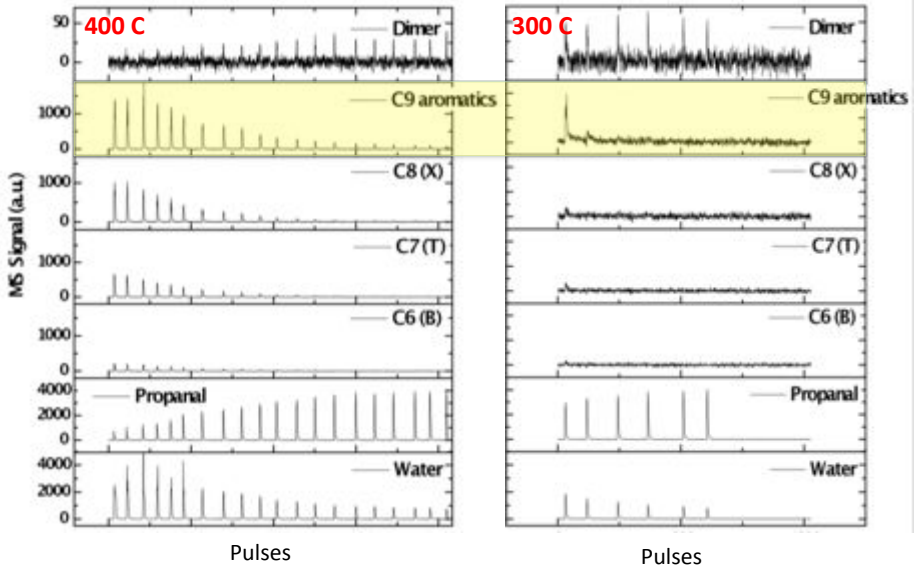

17

Pulses of Propylene on H-ZSM5 produce C6-C7 Aromatics

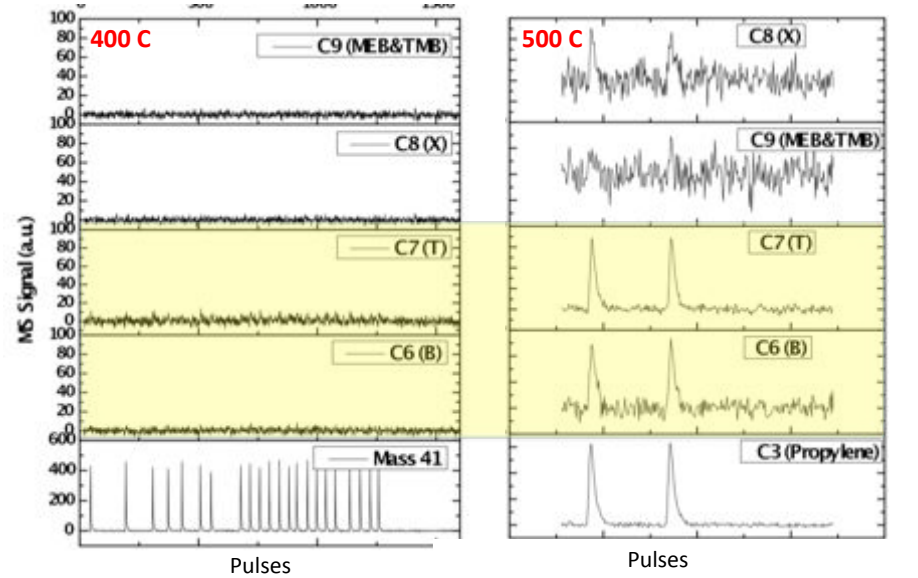

18

Varying Crystallite Size

H-ZSM-5

Si/Al = 45

Crystallite Size ~

< 100 nm

From

Sud Chemie

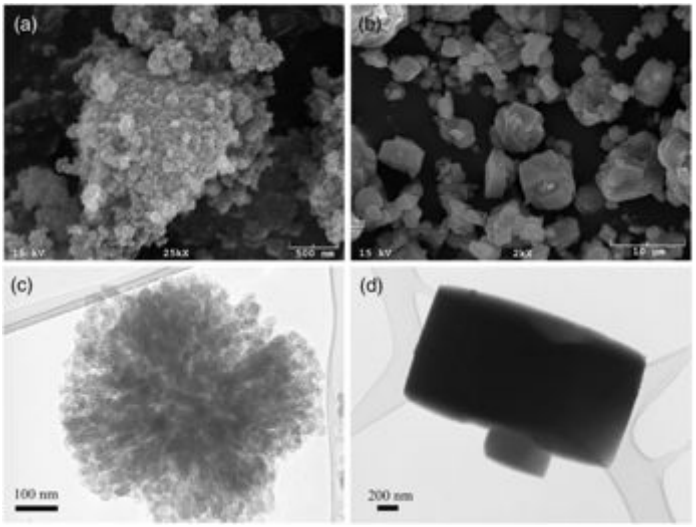

H-ZSM-5

Si/Al = 45

Crystallite Size ~

>1,000 nm

Synthesized In-House

Catalysis Communications 11 (**2010**) 977–981

19

Varying Crystallite Size

H-ZSM-5

Si/Al = 45

Crystallite Size ~

< 100 nm

From

Sud Chemie

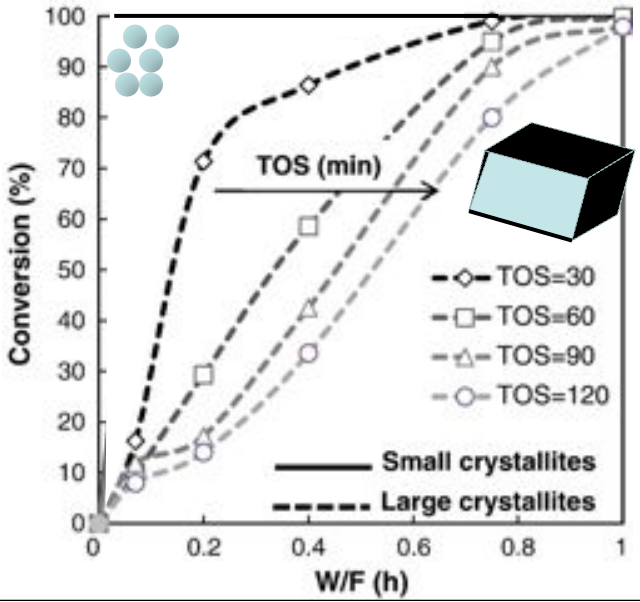

H-ZSM-5

Si/Al = 45

Crystallite Size ~

>1,000 nm

Synthesized In-House

20

Varying Crystallite Size

H-ZSM-5

Si/Al = 45

Crystallite Size ~

< 100 nm

From

Sud Chemie

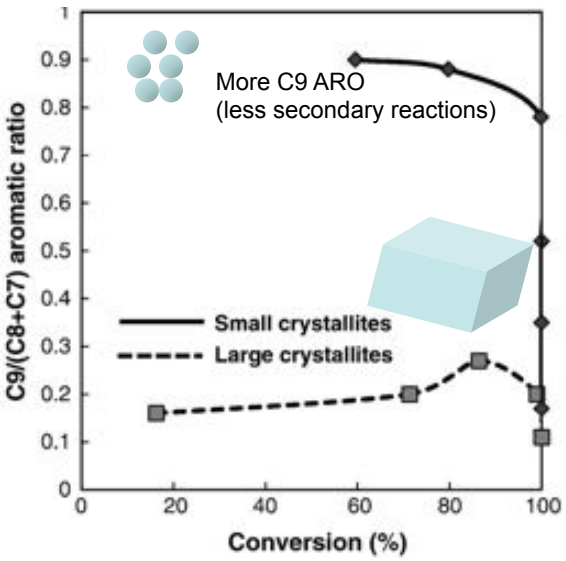

H-ZSM-5

Si/Al = 45

Crystallite Size ~

>1,000 nm

Synthesized In-House

Catalysis Communications 11 (**2010**) 977–981

21

Varying Mesoporous Structure

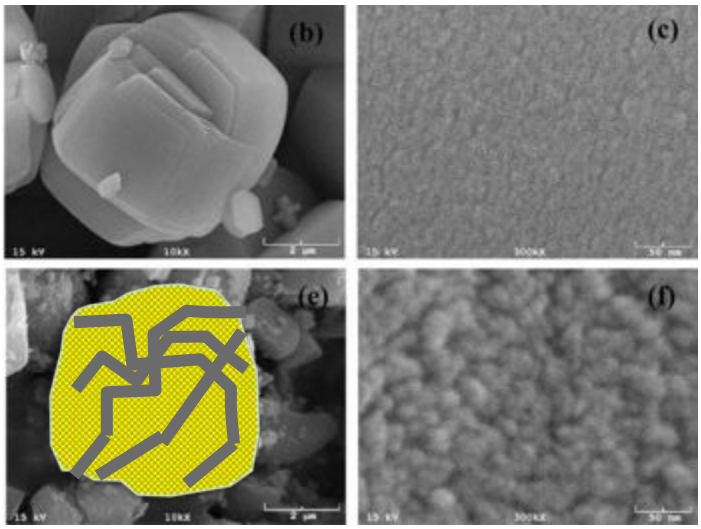

SEM

HZSM-5 catalysts with controlled mesoporosity generated by desilication

Journal of Catalysis 271 (**2010**) 88–98

22

Varying Mesoporous Structure

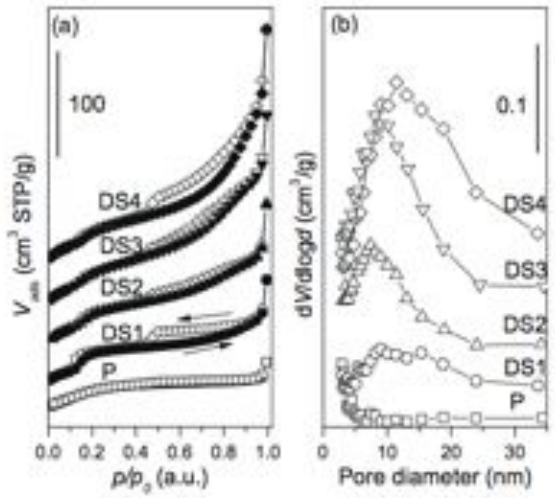

Fig. 3. N_2 adsorption–desorption isotherms (a) and mesopore pore size distributions (b) of parent zeolite (P) and desilicated zeolite samples (DS1 to DS4) of increasing desilication severity.

BET

As the degree of desilication increases, the mesoporosity increases.

J. Catalysis 271 (**2010**) 88–98

Varying Mesoporous Structure

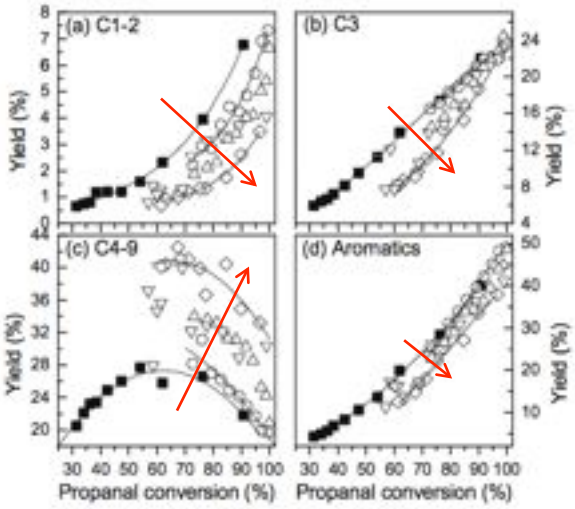

Product Distribution

As mesoporosity increases:

a) Less C1-C3
b) More isoparafins and C4-C9 olefins
c) Slightly less aromatics

Due to reduced residence time inside microcrystalline structure

J. Catalysis 271 (**2010**) 88–98

Strategy No. 2
"Breaking C-O bonds instead of C-C bonds"

Hydro-deoxygenation of Furfural

25

Furfural Conversion on Metal Catalysts

26

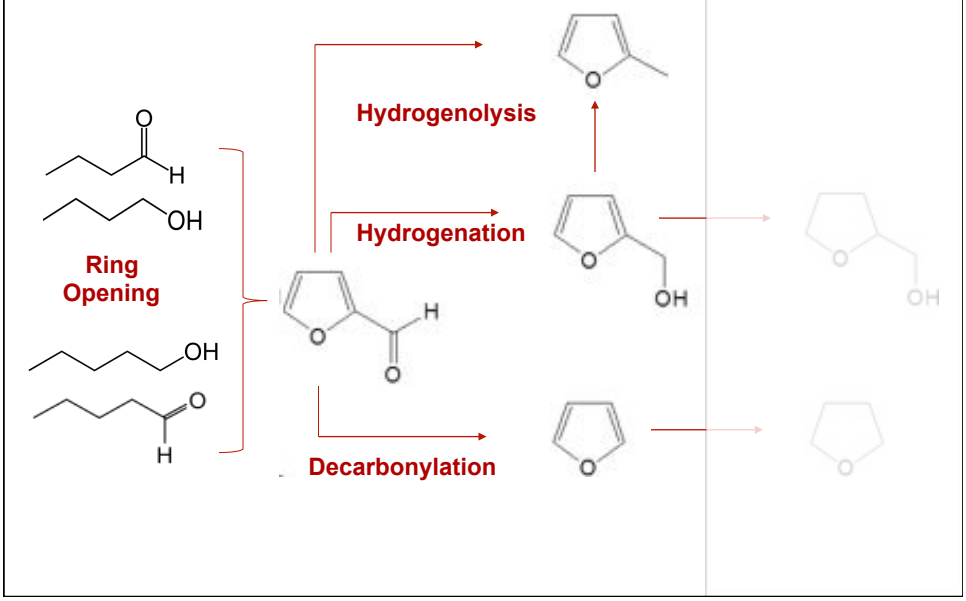

Kinetics. Furfural over Cu/SiO_2

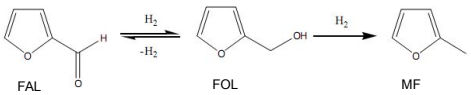

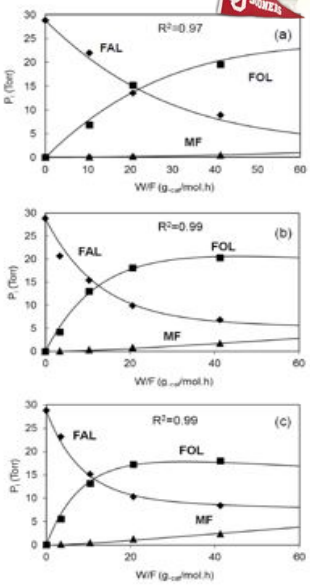

❖ **Langmuir-Hinshelwood model**

$$r_{FAL} = -k_1 K_{FAL} P_{FAL} \theta_V + \frac{k_1}{K} K_{FOL} P_{FOL} \theta_V$$

$$r_{FOL} = k_1 K_{FAL} P_{FAL} - \left[\frac{k_1}{K} K_{FOL} P_{FOL} \theta_V + k_2 K_{FOL} P_{FOL} \theta_V \right]$$

$$r_{2-MF} = k_2 K_{FOL} P_{FOL} \theta_V$$

$$\theta_V = \frac{1}{1 + K_{FAL} P_{FAL} + K_{FOL} P_{FOL} + K_{MF} P_{MF} + K_{H_2}^{1/2} P_{H_2}^{1/2}}$$

Sitthisa , Balbuena, Resasco
J. Catalysis, 277 (2011) 1-13

Kinetics. Furfural over Cu/SiO_2

Table 2. Kinetic and thermodynamic parameters obtained from fitting the experimental data of with the kinetic model at various temperatures

Temp (°C)	Equilibrium constant	Rate constant (mmol/g.cat.h)		Adsorption constant ($Torr^{-1}$)				
	(K_{eq})	k_1	k_2	K_{FAL}	K_{FOL}	K_{MF}	K_{H2}	K_W
230	4.56	3.00	0.10	0.29	0.18	0.083	11.9×10^{-5}	0.25
270	2.98	5.93	0.24	0.12	0.11	0.063	4.2×10^{-5}	0.10
290	2.01	8.05	0.34	0.08	0.09	0.056	2.7×10^{-5}	0.07

$$\ln K = -\frac{\Delta H^{\ominus}}{RT} + \frac{\Delta S^{\ominus}}{R}$$

Heat of adsorption, ΔH_{ads} ($kcal.mol^{-1}$)

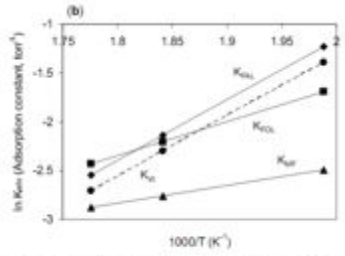

Fig. 7. Rate constants k_1 (a) and adsorption equilibrium constants K_{ads} (b) as a function of inverse temperature.

12.3 6.9 3.7

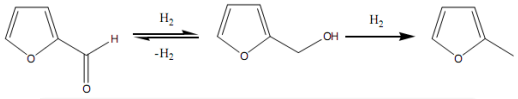

Furfural more strongly adsorbed than furfuryl alcohol and MF.

Sitthisa , Balbuena, Resasco
J. Catalysis, 277 (2011) 1-13

DFT. Furfural over Cu (111)

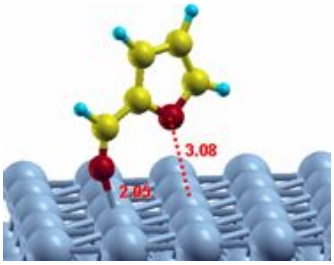

$\Delta H_{ads} < 0$

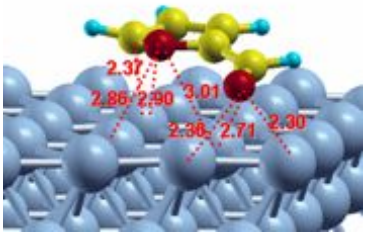

$\Delta H_{ads} > 0$

- Carbonyl perpendicular mode is preferred
- Parallel adsorption modes are not favored (endothermic !)
- Interaction between carbonyl O and surface is main contributor to adsorption strength

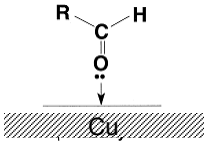

η^1-aldehyde

Sitthisa , Balbuena, Resasco
J. Catalysis, 277 (2011) 1-13

DRIFTS. Furfural over Cu

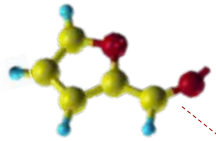

Gas phase

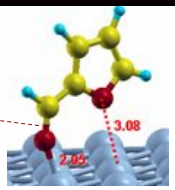

η^1-aldehyde

- Gas phase furfural shows the C=O stretching vibration mode at 1,720 cm^{-1}.

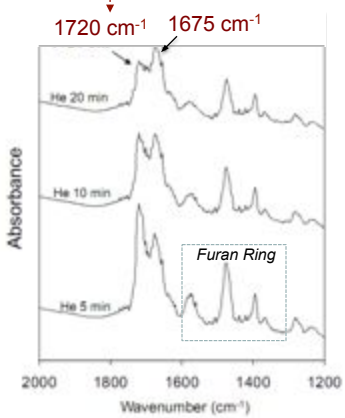

- C=O stretching band in adsorbed furfural appears downshifted from the wavenumber observed for gas-phase furfural.
- Furan ring bands do not change position

Furfural Conversion over Cu/SiO_2

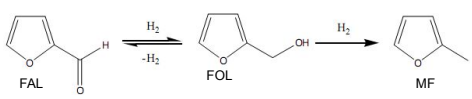

❖ The reaction of furfural (FAL) on Cu/SiO_2 gives mainly furfuryl alcohol (FOL), with MF as a minor product, which is significant only above 230˚C.

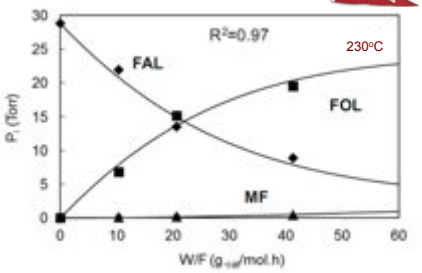

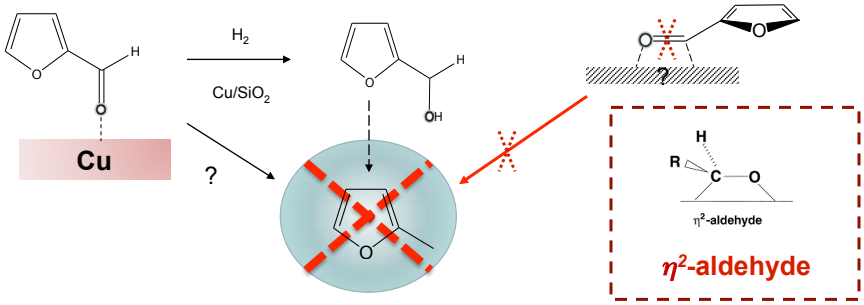

Intermediates on Group VIII Metals

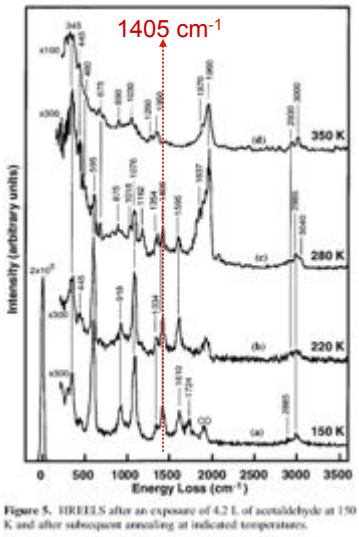

Figure 5. HREELS after an exposure of 4.2 L of acetaldehyde at 150 K and after subsequent annealing at indicated temperatures.

M.A. Barteau J. Phys. Chem. 101 (1997) 7939

❖ preferred mode on Group VIII metals η^2 –aldehyde

❖ η^2 configuration can convert to **acyl**

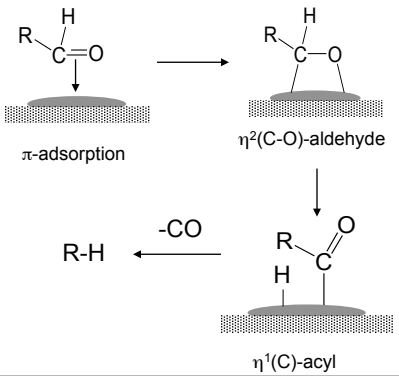

Intermediates on Pd

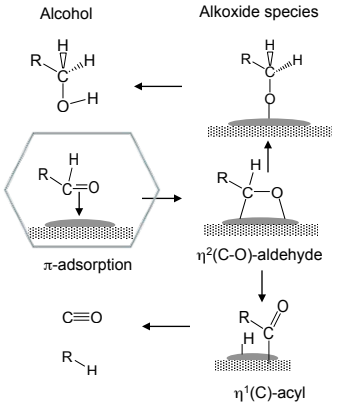

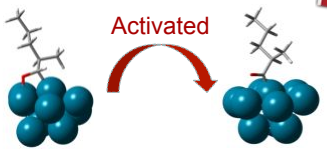

11 kcal/mol

43 kcal/mol

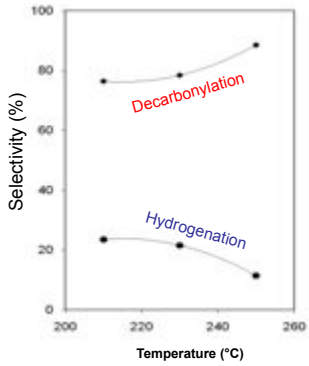

The acyl intermediate becomes dominant at high temperatures

Furfural Conversion over Pd/SiO_2

At T = 230°C

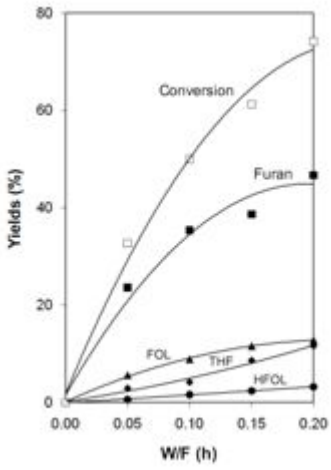

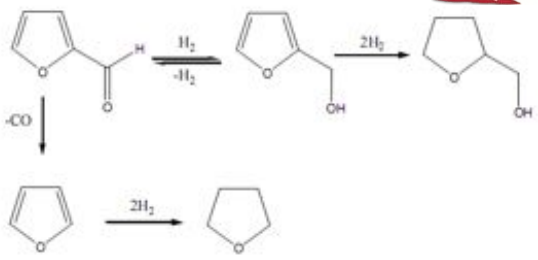

- The main reaction product at every W/F is **furan**, while furfuryl alcohol is observed as a minor product.
- Terahydrofuran (THF) and tetrahydro furfuryl alcohol (HFOL), formed as secondary products, are observed in smaller amounts, and mostly at high W/F.

T = 230C; H_2/feed ratio = 25; TOS 15 min

Decarbonylation of Other Aldehydes

What is the role of the ring ?

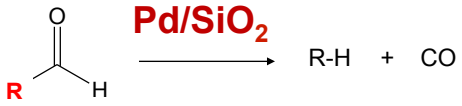

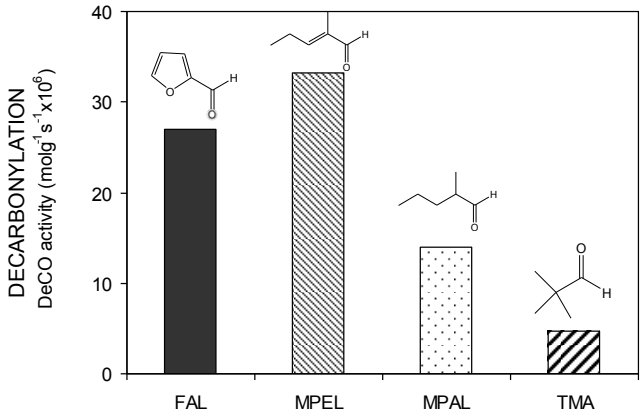

0.006 mole/h of aldehydes, 1%Pd/SiO_2, 250°C, 1 atm, 62.4 ml/min of hydrogen

Decarbonylation of Other Aldehydes

Aldehydes	η^1(C)-Acyl	(DFT) ΔH_{ads} (kcal.mol^{-1})	Activity (μmol. g^{-1}.s^{-1})
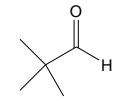	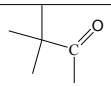	16.3	4.7
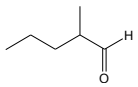	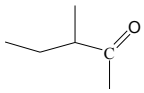	22.0	14.0
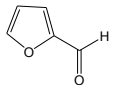	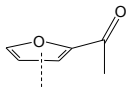	27.5	27.0
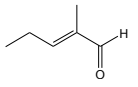	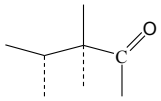	33.4	33.2

Bimetallic Pd-Cu/Silica

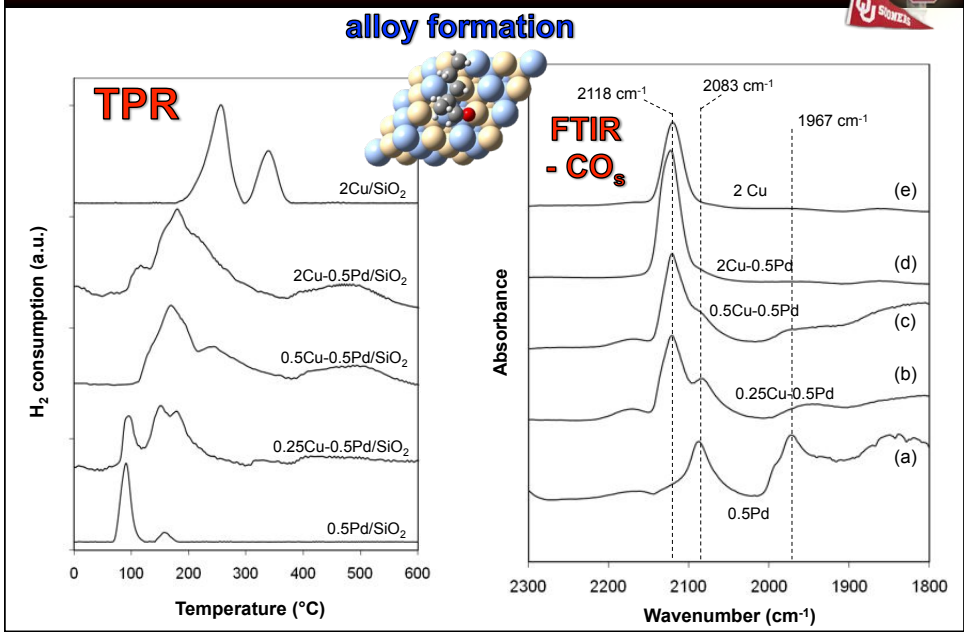

DFT of 2-methyl pentanal (MPAL) on Pd-Cu

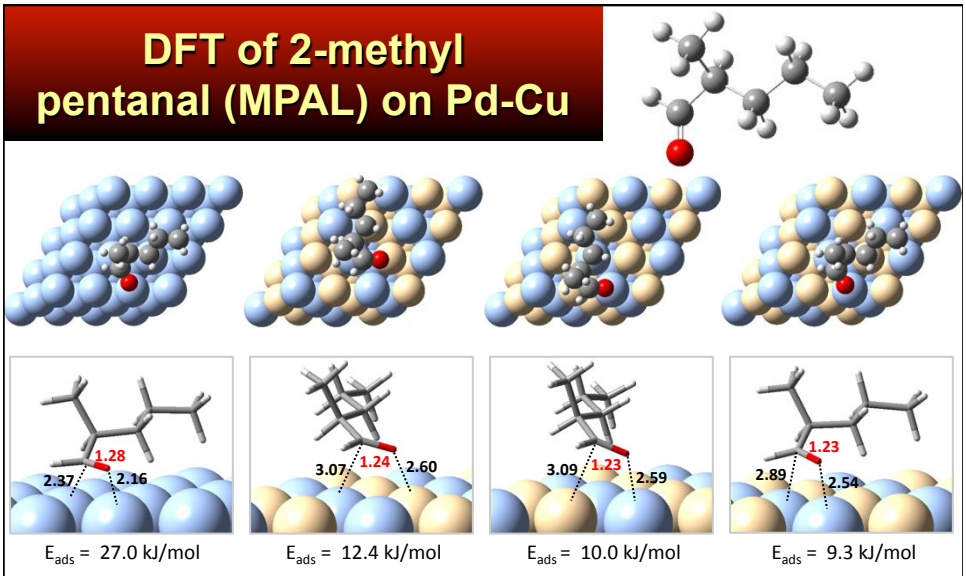

E_{ads} = 27.0 kJ/mol | E_{ads} = 12.4 kJ/mol | E_{ads} = 10.0 kJ/mol | E_{ads} = 9.3 kJ/mol

DFT optimized structures of 2-methylpentanal (MPAL) in gas phase (a), and its adsorption on Pd(111) (b) and PdCu(111) (c-e) slabs. Red, gray, white, blue, and yellow spheres represent O, C, H, Pd and Cu atoms, respectively.

Sitthisa, Pham, Prasomsri, Sooknoi, Mallinson, Resasco, *J. Catalysis*, **280** (2011) 17-27

DFT of 2-methyl pentanal (MPAL) on Pd-Cu

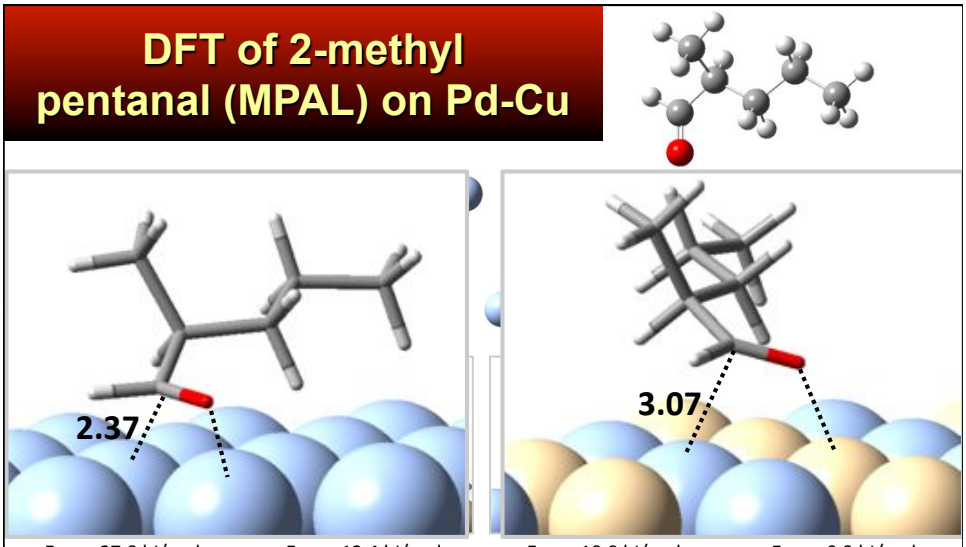

E_{ads} = 27.0 kJ/mol E_{ads} = 12.4 kJ/mol E_{ads} = 10.0 kJ/mol E_{ads} = 9.3 kJ/mol

DFT optimized structures of 2-methylpentanal (MPAL) in gas phase
(a), and its adsorption on Pd(111) (b) and PdCu(111) (c-e) slabs.
Red, gray, white, blue, and yellow spheres represent O, C, H, Pd and Cu atoms, respectively.

Sitthisa, Pham, Prasomsri, Sooknoi, Mallinson, Resasco, *J. Catalysis*, **280** (2011) 17-27

DFT of furfural (FAL) on Pd-Cu

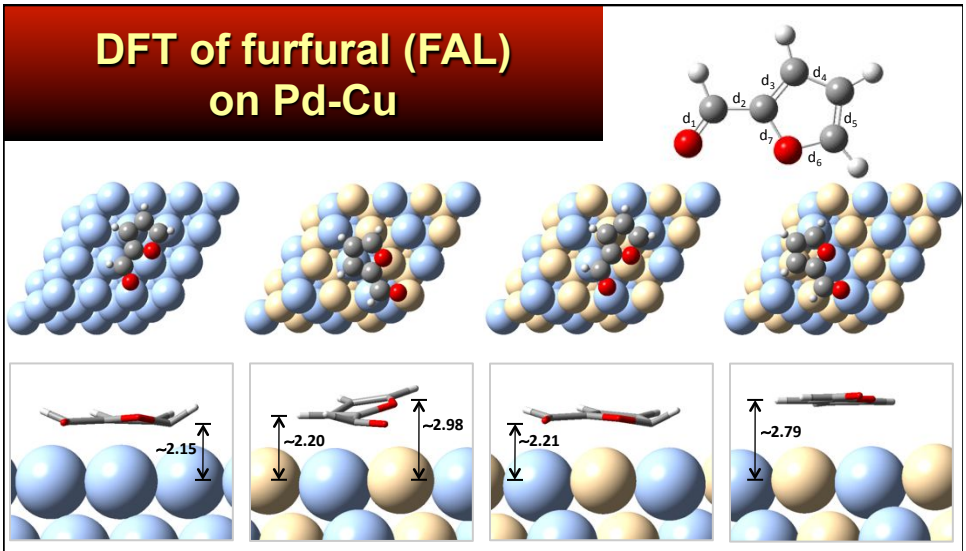

E_{ads} = 55.4 kJ/mol E_{ads} = 9.6 kJ/mol E_{ads} = 7.4 kJ/mol E_{ads} = 4.0 kJ/mol

DFT optimized structures of furfural (FAL) in gas phase
(a), and its adsorption on Pd(111) (b) and PdCu(111) (c-e) slabs.
Red, gray, white, blue, and yellow spheres represent O, C, H, Pd and Cu atoms, respectively.

Sitthisa, Pham, Prasomsri, Sooknoi, Mallinson, Resasco, *J. Catalysis*, **280** (2011) 17-27

Furfural on Pd/SiO_2 and $Pd\text{-}Cu/SiO_2$

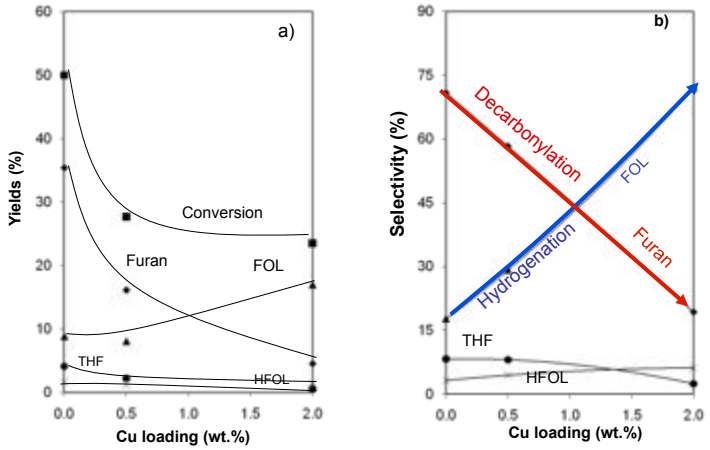

W/F = 0.1 h, Temp = 230°C, H_2/Feed ratio = 25, H_2 pressure = 1 atm, TOS = 15 min

- The total activity for FAL is decreased when the Cu metal was incorporated
- The yield of the decarbonylation products, furan, is greatly reduced while the yield of hydrogenated products (FOL) significantly increases as a function of Cu loading

Furfural on Pd/SiO_2 and $Pd\text{-}Cu/SiO_2$

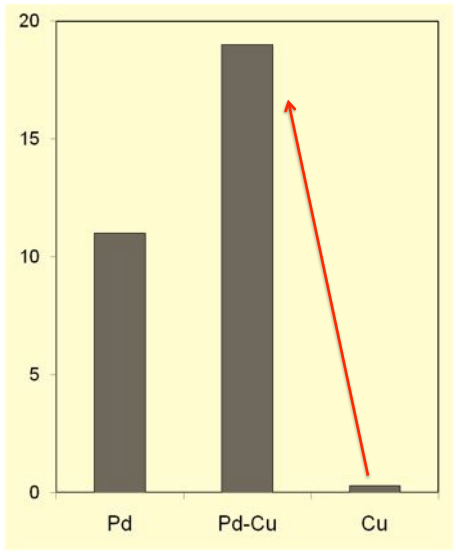

Dramatic increase in ***yield*** of furfuryl alcohol on the Pd-Cu catalyst with high ***selectivity***.

W/F = 0.2 h, Temp = 250°C, H_2/Feed ratio = 25, Pressure = 1atm, TOS = 15 min.

Sitthisa, Pham, Prasomsri, Sooknoi, Mallinson, Resasco, *J. Catalysis*, **280** (2011) 17-27

Furfural on Pd/SiO_2 and $Pd-Fe/SiO_2$

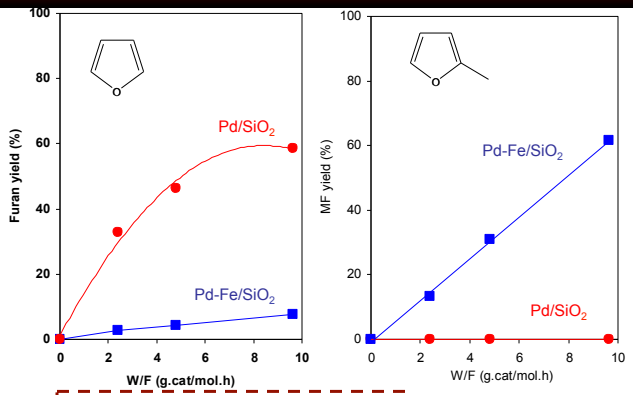

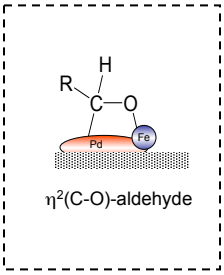

η^2(C-O)-aldehyde

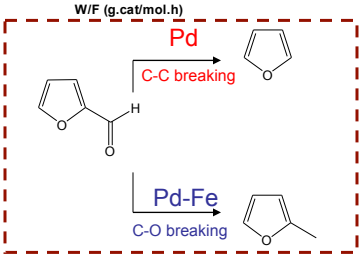

- Decarbonylation dramatically decreased when Fe was added to Pd.
- 2-methyl furan became the main product over Pd-Fe catalyst.

Furfural on Ni/SiO_2 and $Ni-Fe/SiO_2$

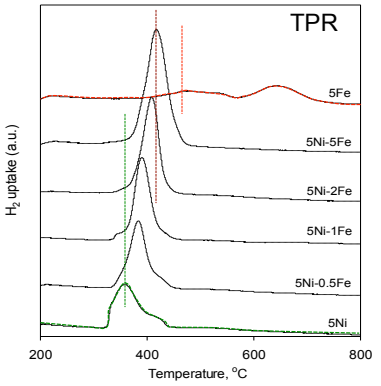

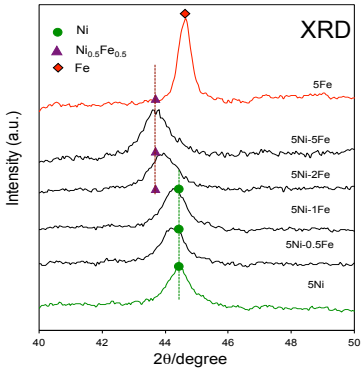

Catalysts	lattice constant (Å)	
	XRD	DFT
5Ni	3.53	3.52
5Ni-5Fe	3.58	3.55
5Fe	2.87	2.87

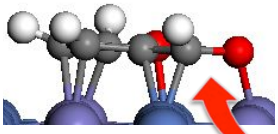

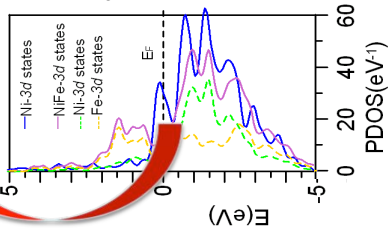

Furfural on Ni/SiO_2 and $Ni-Fe/SiO_2$

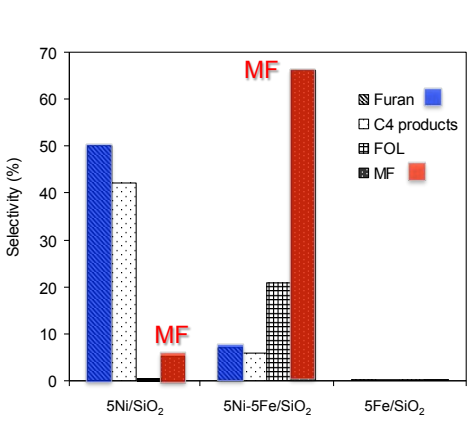

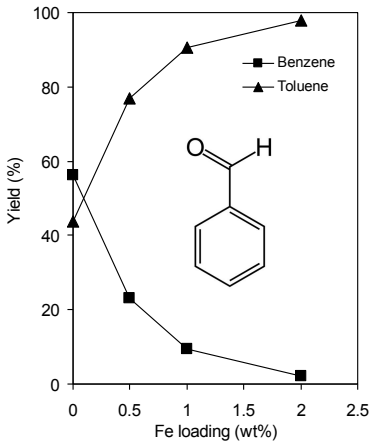

Ni (decarbonylation) ➔ **Ni-Fe** (hydrogenolysis)

Furfural Conversion on Metal Catalysts

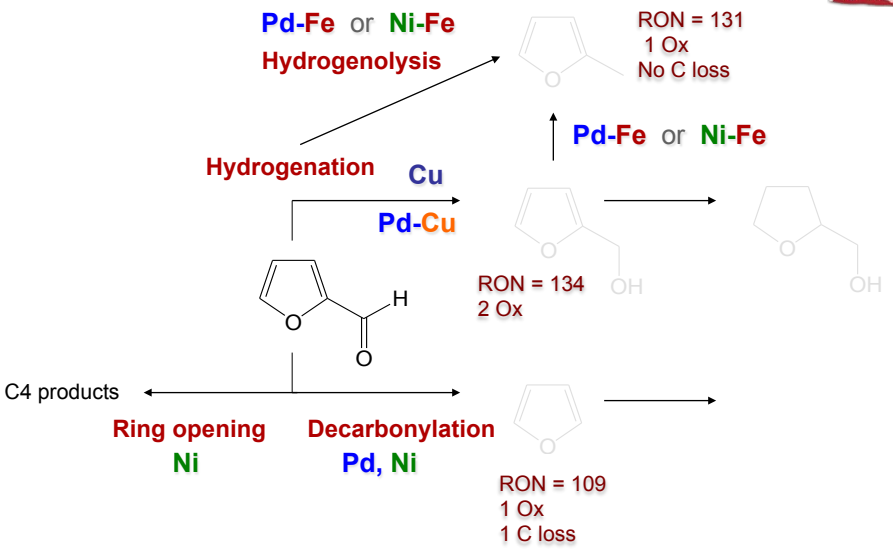

Strategy No. 3

Multi-functional Catalysis
in Bi-Phasic Liquid Systems
Stabilized by Nanoparticles

47

Conversion in Liquid Phase (biphasic)

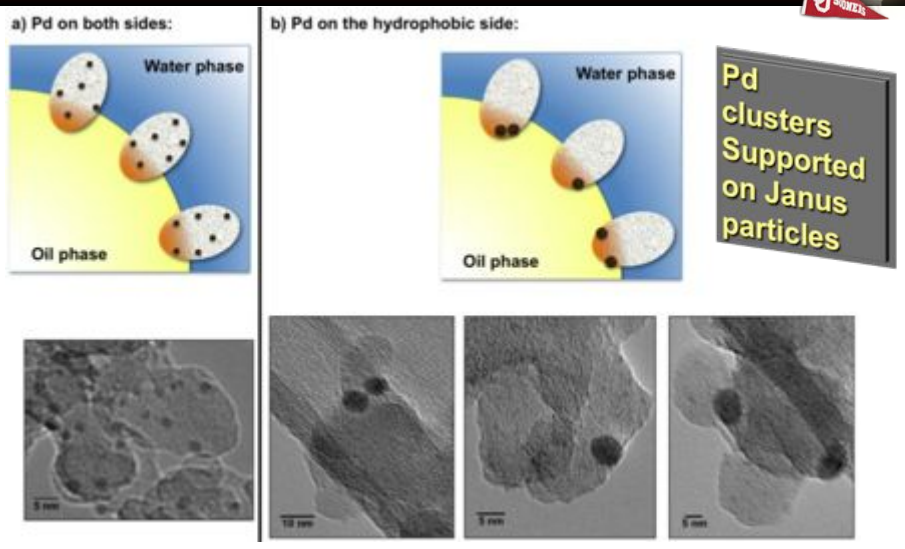

Advanced Synthesis and Catalysis **2010**, 352, 2359 – 2364

48

Rates only depend on thermodynamic activities of reactants and products

Reactions on surfaces do not detect the presence of contacting fluid, unless:

a. Mass transport limitations (changes in local chemical potential)
b. Competitive adsorption
c. Solvation of kinetically relevant intermediates

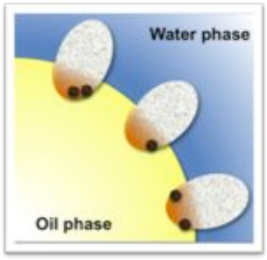

Therefore, phase selectivity in emulsions only due to a, b, c

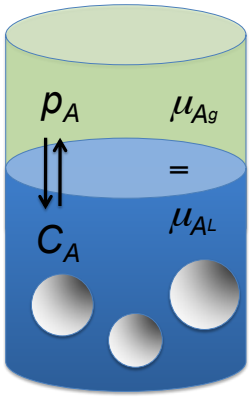

R. J. Madon, E. Iglesia, J. Molecular Catalysis A: Chemical 163 (2000) 189

Conversion in Liquid Phase (biphasic)

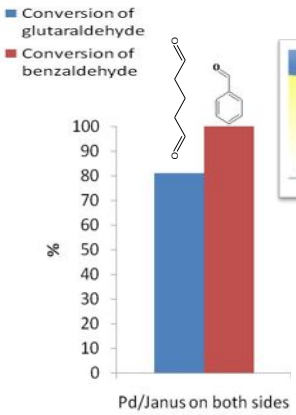

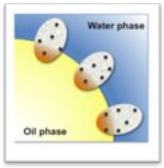

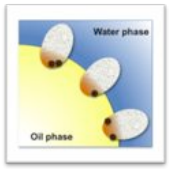

Semi-batch reactor at T=100ºC continuous flow of H_2 110 sccm through liquid at P= 200 psi; 0.03 g catalyst , reaction time 3 h.

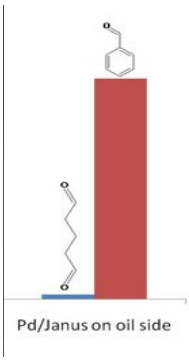

Advanced Synthesis and Catalysis **2010**, 352, 2359 – 2364

Condensation of Oxygenates on MgO/CNT/Pd

STEP 2:
Temperature Staged Hydrogenation

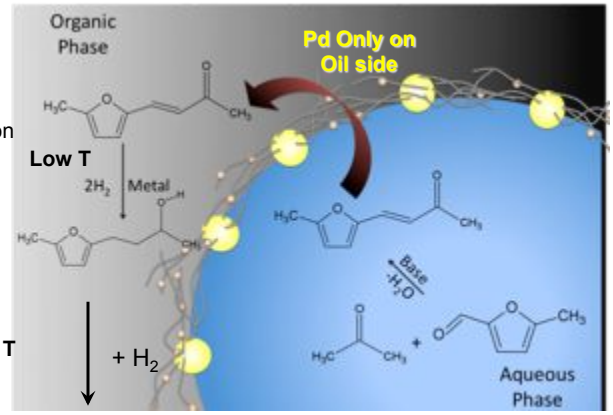

Crossley, Sen, Faria, Resasco SCIENCE, 327, 68-72 **(2010)**

STEP 1:
Based-catalyzed aldol condensation:
- MgO nanoparticles
- Na(OH) homogeneous

Importance of ***Phase Selectivity***
To Maximize Yield

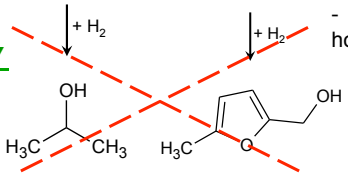

Need to hydrogenate in oil phase ONLY

Strategy No. 4
"Eliminate O while keeping C in the fuel range"

Selective Hydro-Deoxygenation of Phenolic Compounds

52

Lignin-derived Phenolics

Oxygenated aromatics

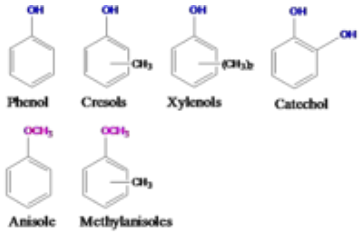

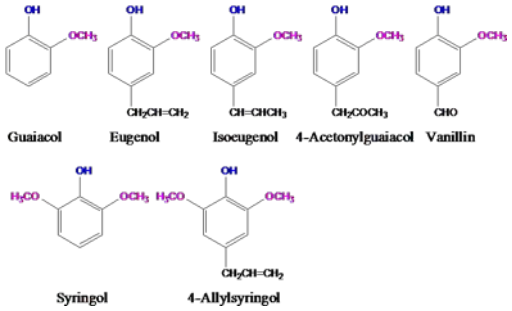

Industrial Approaches ⇒
- **Co-processing in FCC units**
- **Severe HDT**

Alternative: ⇒ **Mild hydrotreating (remove O, keep C)**

Conversion of Anisole - Acid Catalyst

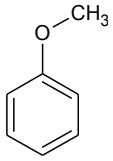

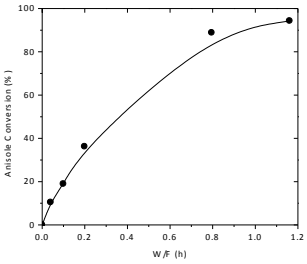

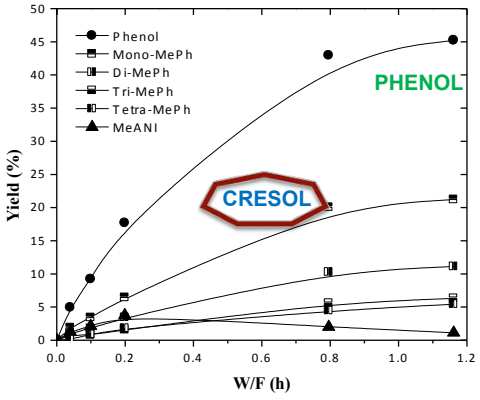

Effect of space time (W/F) on anisole conversion over amorphous SILICA-ALUMINA
Reaction conditions: T = 300 °C, P = 1 atm, TOS = 10 min.

Trans-Alkylation of Anisole

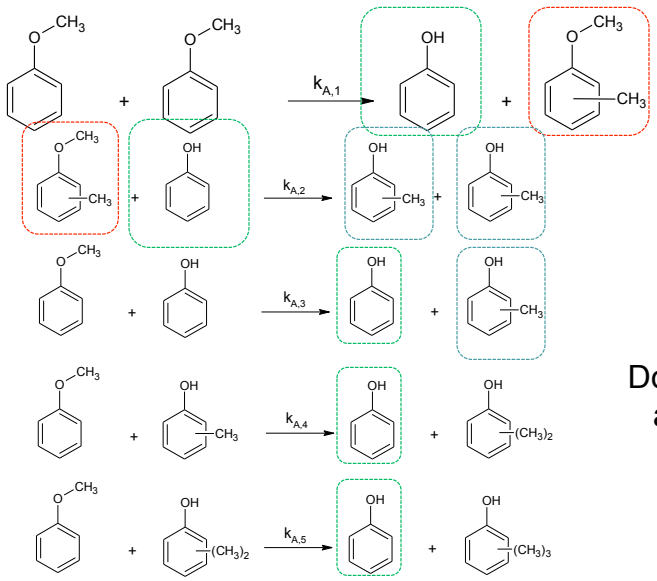

Dominant products are Phenol and Cresol

Conversion of Guaiacol - Acid Catalyst

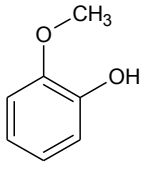

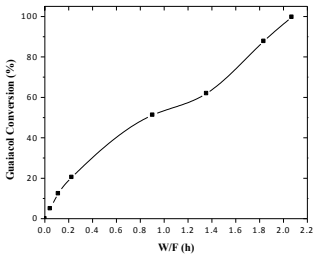

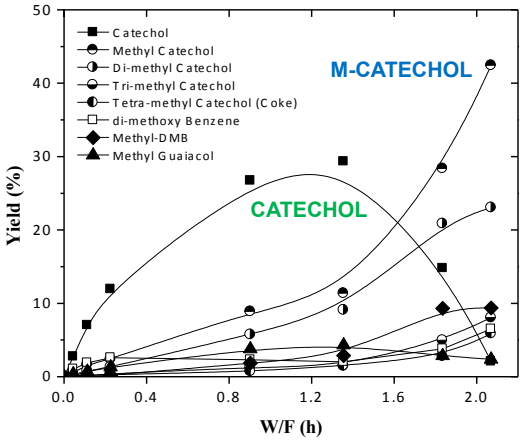

Effect of space time (W/F) on guaiacol conversion over amorphous SILICA-ALUMINA
Reaction conditions: T = 300 °C, P = 1 atm, TOS = 10 min.

DFT - Anisole and Guaiacol Adsorption
(Brønsted/Lewis Acid Sites)

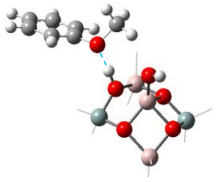

ANI on B-acid
-22.8 kcal/mol

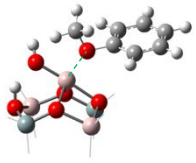

ANI on L-acid
-27.7 kcal/mol

Catalyst site	Heat of Adsorption (kcal/mol)	
	Anisole	Guaiacol
Bronsted	-22.8	-27.8
Lewis	-27.7	-30.5
Bronsted and Lewis	N/A	-49.3

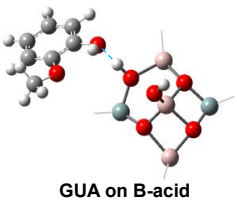

GUA on B-acid
-27.8 kcal/mol

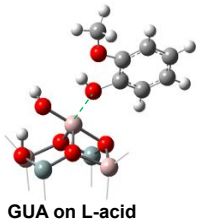

GUA on L-acid
-30.5 kcal/mol

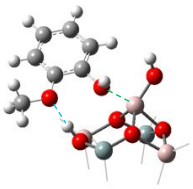

GUA on B/L-acid
-49.3 kcal/mol

Temperature Programmed Desorption

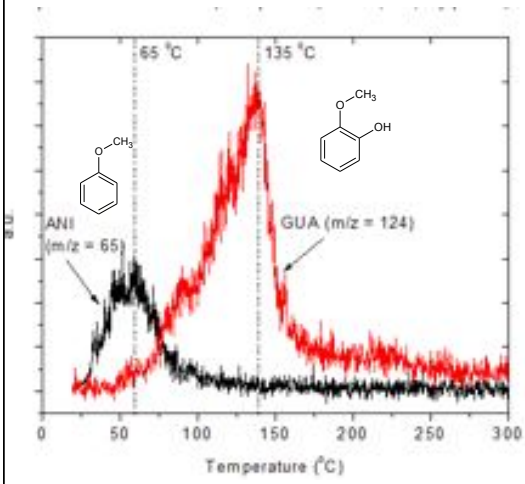

TPD Anisole and Guaiacol after chemisorption at room temperature.

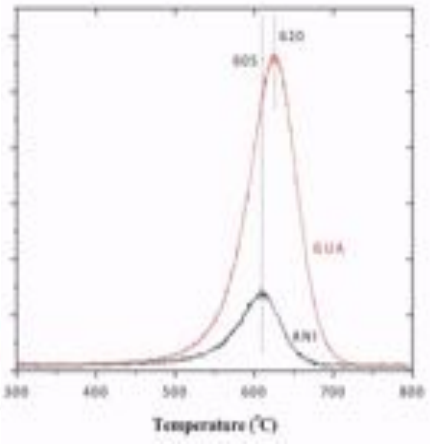

TPO after the TPD of Anisole and Guaiacol chemisorbed at room temperature.

Anisole Vs. Guaiacol

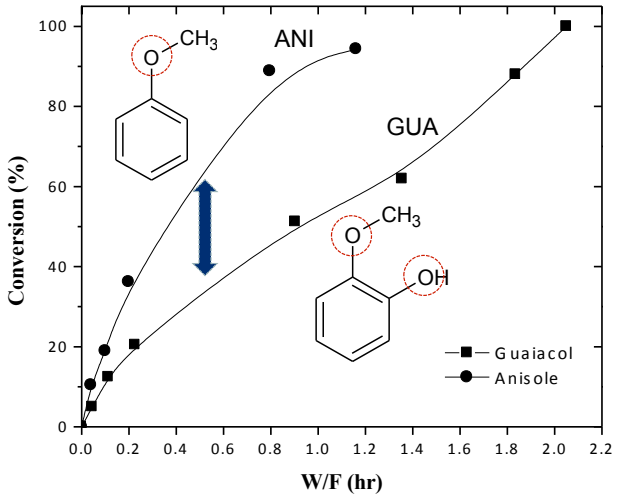

Guaiacol should be more reactive.

Faster deactivation ?

Effect of space time (W/F) on conversion of anisole and guaiacol over amorphous **SILICA-ALUMINA**
Reaction conditions: Temp = 300 °C, P = 1 atm, TOS = 10 min.

Anisole Vs. Guaiacol

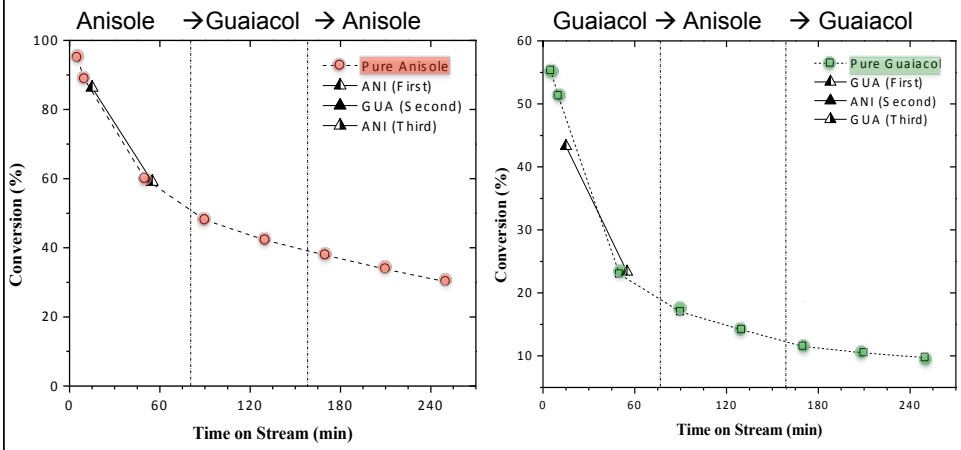

Effect of switching anisole and guaiacol feeds over amorphous **SILICA-ALUMINA** – W/F = 1
Reaction conditions: Temp = 300 °C, P = 1 atm

Effect of co-feeding hydrocarbons

Oxygenates: **Anisole** *(Bio-oil model compound)*

Co-feeds: **Tetralin** *(good H-donor)*
n-Decane
Benzene
Propylene

Catalysts: HY zeolites (Si/Al=15 and 40)
Temp: 400 ºC
Pressure: 1 atm He

Relative hydrogen transfer ability: DFT study

DMT > tetralin > decalin > n-decane

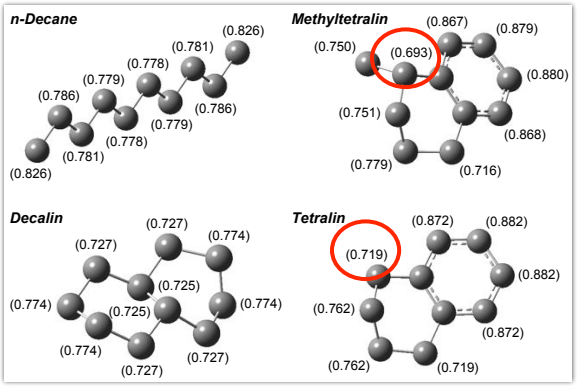

T. Prasomsri, R. E. Galiasso, W. E. Alvarez, T. Sooknoi, D. E. Resasco, *Appl. Catal. A*, 389, 140-146, **2010**

Conversion of Pure Anisole

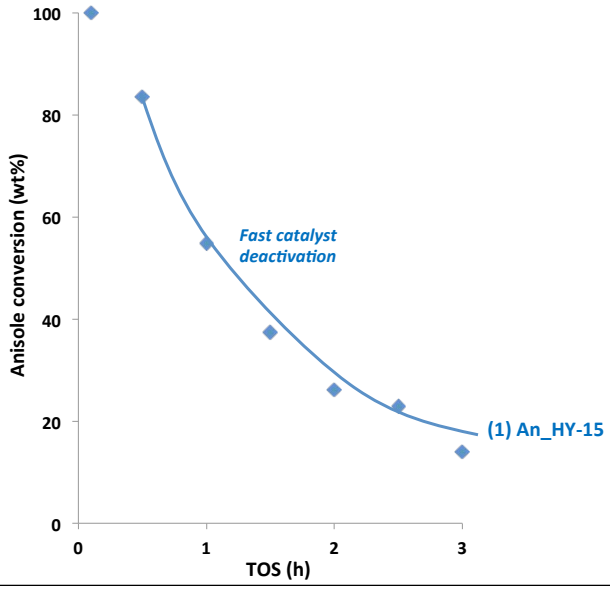

Reaction Conditions:
- W/F = 0.419 h
- Temp = 400 C
- Pressure = 1 atm
- He flow = 40 cc/min

***NOTE:** Thermal conversion of An/Tet is negligible*

"Catalytic conversion of anisole over HY and HZSM-5 zeolites in the presence of different hydrocarbon mixtures," T. Prasomsri, Anh T. To, S. Crossley, W. E. Alvarez, D. E. Resasco, *Appl. Catal. B:* 106, 204-211, **2011**

Conversion of Anisole in Mixed Feeds

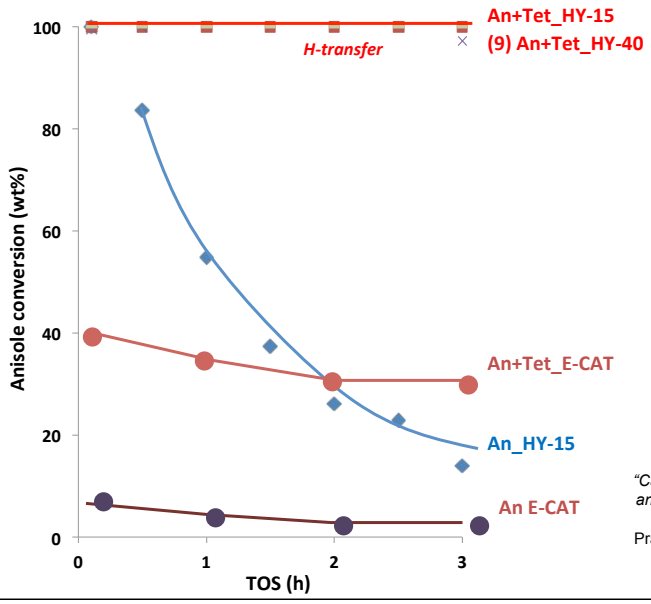

Reaction Conditions:
- W/F wrt. Anisole = 0.419 h
- Temp = 400 C
- Pressure = 1 atm
- He flow = 40 cc/min

***NOTE:* Thermal conversion of An/Tet is negligible**

"Catalytic conversion of anisole over HY and HZSM-5 zeolites in the presence of different hydrocarbon mixtures," T. Prasomsri, Anh T. To, S. Crossley, W. E. Alvarez, D. E. Resasco, *Appl. Catal. B:* 106, 204-211, **2011**

Anisole conversion over H-Beta

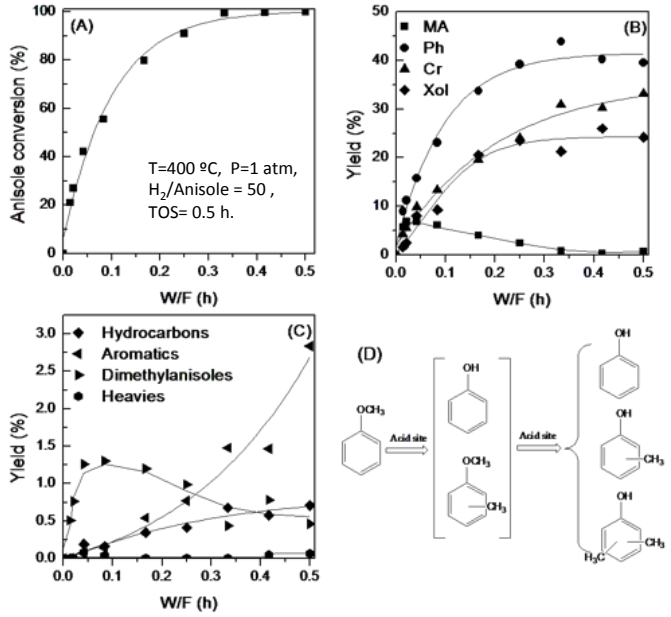

- Yield of hydrocarbons is very small.
- The major reaction is transalkylation.

PHENOL CRESOL AND XYLENOL ARE DOMINANT PRODUCTS

Bifunctional transalkylation and hydrodeoxygenation of anisole over a Pt/HBeta catalyst X. Zhu, L. Lobban, R.G. Mallinson, D.E. Resasco *J. Catalysis*, 281, 21-29, **2011**

Anisole conversion over 1% Pt/SiO_2

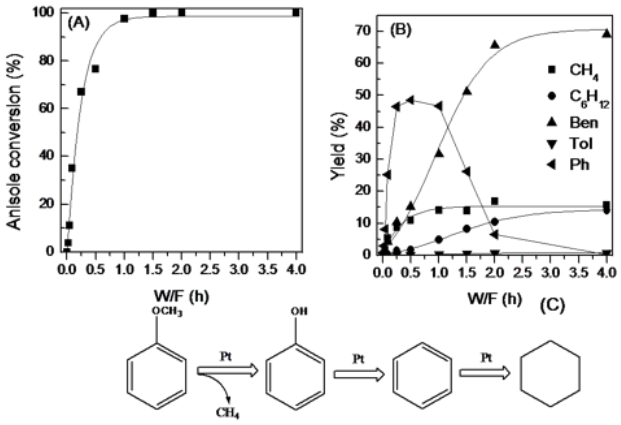

- One carbon is lost by methane formation.
- Phenols is the primary product, and can be hydrodeoxygenated to benzene.
- Benzene can be further hydrogenated to cyclohexane which is undesirable.

Bifunctional transalkylation and hydrodeoxygenation of anisole over a Pt/HBeta catalyst
X. Zhu, L. Lobban, R.G. Mallinson, D.E. Resasco
J. Catalysis, 281, 21-29, **2011**

Reaction conditions: T=400 ºC, P=1 atm, H_2/Anisole=50, TOS= 0.5 h.

Anisole conversion over 1% Pt/H-Beta

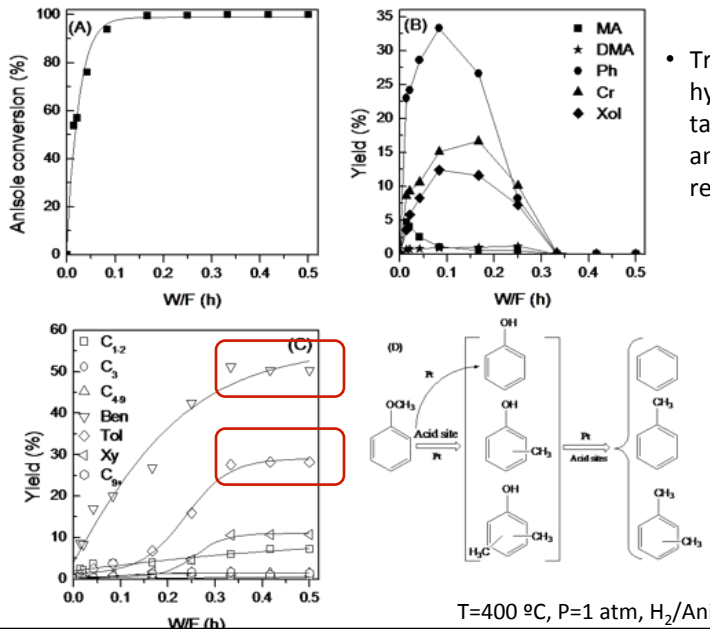

- Transalkylation and hydrodeoxygenation take place over acid and metal sites, respectively.
  - Yields of hydrocarbons is enhanced significantly
  - The carbon number is preserved.

T=400 ºC, P=1 atm, H_2/Anisole=50, TOS= 0.5 h.

Summary

- Upgrading of bio-oil with maximum yield and minimum oxygen is a challenging task >> It needs multi-stage solution.
- Studies with model compounds are valuable to identify different catalytic strategies
- Oxygen functionalities (-OH, -OCH_3, C=O) can be used to enlarge C-C backbone chain
- Oxygen functionalities are highly deactivating of catalysts. Hydrogen usage is important.
- Liquid-phase processes (biphasic) offer promise for operating at milder conditions and minimize hydrogen consumption

Acknowledgements

Faculty:

R. G. Mallinson; T. Sooknoi; L. L. Lobban; F. Jentoft; R. Jentoft; P. Balbuena

Students and Post-docs:

Trung Hoang, Xinli Zhu, Surapas Sitthisa, Ming Sen, Teerawit Prasmosri, Sunya Boonyasuwat, Tu Pham, Jimmy Faria, Pilar Ruiz, Paula Zapata.

Funding

- Department of Energy - National Science Foundation / EPSCOR - Oklahoma Bioenergy Center - State Grant

Is Phase Selectivity (thermodynamically) possible ?

Phase 1		Phase 2
	$\mu_A^1 = \mu_A^2$	
	$f_A^1 = f_A^2$	
$r_A = ka_A^1$		$r_A = ka_A^2$
	$a_A^1 = a_A^2$	
	$\gamma_A^1 c^1 = \gamma_A^2 c^2$	
$r_A^1 = (k\gamma_A^1)c_A^1$		$r_A^2 = (k\gamma_A^2)c_A^2$

$$r_A^1 = r_A^2$$

The rates should be the same no matter the location of the reactants ….. *UNLESS*

Mass Transport Effects

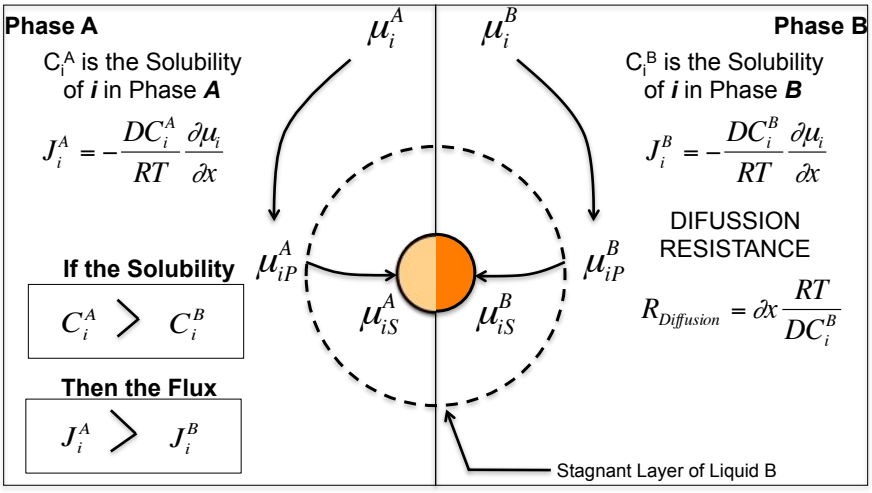

Mass Transport Effects

Organic molecules from the oil droplets in the O/W emulsion to oil on the single phase

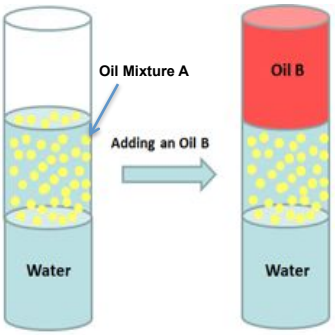

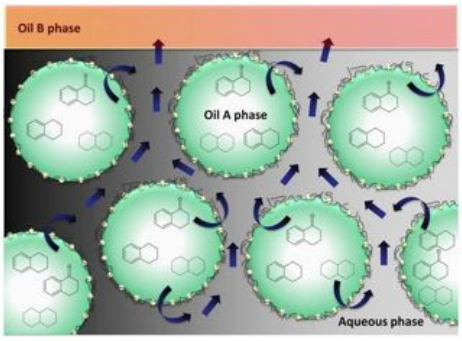

Oil Inside the Droplets: Tetralone + Decalin
Oil B: Tetralin
Aqueous Phase: DI Water

LogP of Tetralone = 2.24
Log P of Decalin = 3.88
Log P of Tetralin = 3.15

Mass Transport Effects

Stagnant System

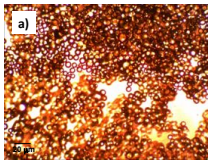

Under Stirring (200rpm)

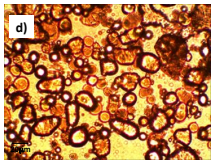

LogP of Tetralone = 2.24
Log P of Decalin = 3.88
Log P of Tetralin = 3.15

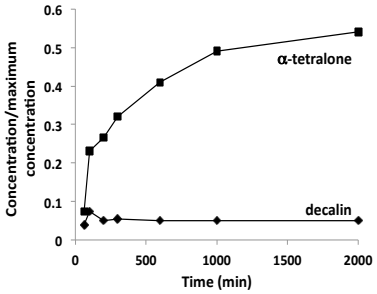

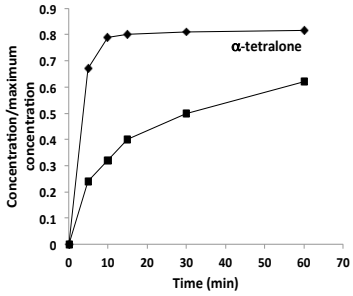

Crossley S, Faria J, Shen M, *Resasco* D.E, *SCIENCE*, **327**, 68-72 (2010)

Ni-Fe Phase Diagram